Intermetallics 87 (2017) 55–60

Contents lists available at ScienceDirect

Intermetallics

journal homepage: www.elsevier.com/locate/intermet

Ab initio calculations of structural and magnetic properties of Ni-Co-Mn-Cr-Sn supercell

Mikhail A. Zagrebin[a,b,*], Vladimir V. Sokolovskiy[b,c], Vasiliy D. Buchelnikov[a]

[a] Chelyabinsk State University, 454001 Chelyabinsk, Russia
[b] National Research South Ural State University, 454080 Chelyabinsk, Russia
[c] National University of Science and Technology "MIS & S", 119991 Moscow, Russia

ARTICLE INFO

Keywords:
Functional alloys (magnetic, electrical, biomedical)
Density functional theory
Magnetic properties
Martensitic transformation
Ab initio calculations

ABSTRACT

The crystal lattice parameters, tetragonality degree, magnetic moments, magnetic exchange parameters in the $Ni_7Co_1Mn_5Cr_1Sn_2$ Heusler alloy are investigated by *ab initio* calculations and supercell approach. Three 16-atom supercells with different atomic configurations relative to Cr atom are considered. On the one side, if the Cr atom is surrounded by one Sn and two Mn nearest neighbors the respective supercell in austenite is found to be favorable with compared to other ones. On the other side, the supercell consisting three nearest Mn atoms against Cr atom is more stable in martensite. Total magnetic moment of all supercells is almost the same and it increases linearly with increasing lattice parameter. Exchange interactions between Cr and Mn atoms depend strongly on the atom distribution. The strong antiferromagnetic coupling between nearest Cr-Mn pairs is found.

1. Introduction

Nowadays, a new class of ferromagnetic (FM) shape-memory alloys (e.g., Co-doped Ni-Mn-(Ga, In, Sn)) has received considerable attention due to a variety of magnetic, mechanical and thermal properties which are associated with a coupled magnetostructural first-order phase transition [1–3]. This transition occurs from the magnetically weak martensite to ferromagnetic austenite during heating and can take place near the room temperature region. As a result, the Co-doped NiMn-based Heusler alloys could be promising for prospective applications, such as a magnetic cooling technology and as a magnetic sensor [1–3].

In addition to experimental researches the numerous first-principles studies aiming to understand the ground state properties of off-stoichiometric Co-doped Ni-Mn-based Heusler alloys have been performed in recent years [4–8]. As it is well known one of the way to create an off-stoichiometric composition is the supercell approach which allows us to get more accurate information about the structural and magnetic properties of solids. In Ref. [4] the composition-dependent crystal structure, elastic and magnetic properties of $Ni_{2-x}Co_xMn_{1.60}Sn_{0.40}$ ($0 \leq x \leq 0.50$) has been studied by using first-principles calculations. It has been shown that the martensitic phase transformation is accompanied with transition from FM state to the antiferromagnetic (AF) one. Lattice parameter, elastic modulus and energy difference between the FM austenite and the AF martensite depend on the Co addition [4]. A. Grünebohm et al. [5] have studied the ground state properties of Ni-Co-Mn-Sn and shown that there is a multitude of local minima in the energy landscape which belong to different ferromagnetic (FIM) states and are close in total magnetization and energy. The effect of Cr atom on the structural, magnetic and magnetocaloric properties of Ni-Co-Mn-In alloy has been recently studied by using jointly *ab initio* and Monte Carlo methods [6–8]. It was shown that the substitution of 5% Co for Ni and 5% Cr for Mn results in a first-order magnetostructural transition from ferromagnetic austenite to antiferromagnetic martensite. As a result, a large change in magnetization and giant inverse magnetocaloric effect ($\Delta T_{ad} \approx 10$ K at $\Delta H = 2$ T) were predicted [8].

The present work is devoted to detailed investigation of magnetic and structural properties of Cr-doped Ni-Co-Mn-Sn alloy by using the 16-atom supercell approach with a different atomic distribution against Cr atom.

2. *Ab initio* calculation details

The ground state and geometry structure optimization calculations have been performed by using the *ab initio* total-energy and molecular dynamics program VASP (Vienna *ab initio* simulation program) developed at the Fakultät fur Physik of the Universität Wien [9,10]. The interaction between ions and electrons was described the projector-augmented wave (PAW). The generalized gradient approximation (GGA) in Perdew-Burke-Ernzerhof (PBE) parametrization [11] was used to

* Corresponding author. Chelyabinsk State University, 454001 Chelyabinsk, Russia.
E-mail address: miczag@mail.ru (M.A. Zagrebin).

http://dx.doi.org/10.1016/j.intermet.2017.04.004
Received 2 December 2016; Received in revised form 30 March 2017; Accepted 5 April 2017

describe the exchange-correlation energy and up to now it is the best approach to describe the magnetic materials. For the pseudopotentials used, the electronic configurations are Ni($3p^6 3d^8 4s^2$), Co($3d^8 4s^1$), Mn ($3p^6 3d^5 4s^2$), Cr($3p^6 3d^5 4s^1$), and Sn($4d^{10} 5p^2 5s^2$), respectively. The kinetic energy cut-off was 400 eV and the kinetic energy cut-off for the augmentation charges was 800 eV. A Monkhorst-Pack grid [12] was employed to sample the Brillouin zone. The *k*-points in the Brillouin zone for self-consistent field cycles were generated with 12^3 meshes for the tetragonal distortion (c/a) and lattice relaxation calculations. The performed calculations were semirelativistic and the spin polarization was taken into account for all the cases. To calculate the tetragonal distortions of the cubic structure, we fixed the volume of a supercell as $V_0 = a^3{}_0 \approx a^2 c$. For the optimized lattice parameter, the Heisenberg's magnetic exchange coupling parameters J_{ij} were calculated using the spin-polarized relativistic Korringa-Kohn-Rostoker (SPR-KKR) package [13] with account of the GGA-PBE functional. This code is based on the KKR-Green's function formalism that makes use of the multiple-scattering theory, and the electronic structure is expressed in terms of the corresponding Greens function as opposed to Bloch wave functions and eigenvalues. The exchange coupling parameters J_{ij} within a real-space approach were calculated using an expression proposed by Liechtenstein et al. [14].

The $L2_1$ crystal structure with space group of Fm-3m (225) which consists of four interpenetrating face-centered cubic sublattices was taken into consideration. In this structure the Sn atoms occupy the sites (0; 0; 0); Mn occupy (1/2; 1/2; 1/2) ones; Ni and Co atoms are randomly located at the sites (1/4; 1/4; 1/4) and (3/4; 3/4; 3/4). The location of addition of Mn and Cr atoms was assumed to be at Sn-site [8]. It should be noted that we will use follow designations such as Mn_Y and Mn_Z. Here, Mn atoms located at regular Mn sublattice are denoted as Mn_Y, whereas Mn_Z designation corresponds to Mn atoms occupied the Sn sublattice. We considered three different types of $Ni_7Co_1Mn_5Cr_1Sn_2$ supercell, as shown in Fig. 1.

For supercells #1 and #2 one Cr atom is placed to Mn_Y regular sublattice, while in a case of supercell # 3 one Cr atom is located at Sn sublattice. It can be observed that in a case of first (second) supercell the Cr atom is surrounded by two (one) Sn and one (two) Mn nearest neighbors, respectively. Opposite, for the third supercell one Cr atom has three nearest Mn atoms.

Besides, *ab initio* calculations have been carried out for four magnetic configurations schematically presented in Fig. 2 and referred as the FM state (all magnetic moments of Ni, Co, Cr, Mn_Y, and Mn_Z are parallel) and three FIM states: FIM-I (spin of Cr on either *X*, *Y* or *Z* lattice is reversed), FIM-II (spins of Mn_Z are reversed), and FIM-III (spins of Mn_Z and Cr are reversed). Since the Sn atom has a small magnetic moment, hence it was not taken into account.

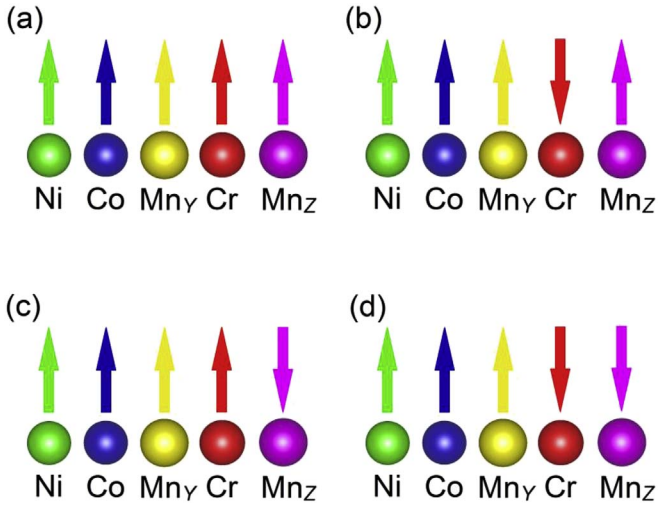

Fig. 2. Different magnetic configurations of $Ni_7Co_1Mn_5Cr_1Sn_2$ taken into account in *ab initio* calculations. a) FM; b) FIM-I; c) FIM-II; d) FIM-III. (For interpretation of the references to colour in this figure legend, the reader is referred to the web version of this article.)

3. *Ab initio* calculation results

3.1. Reference states

In order to find the optimized lattice parameters of Ni-Co-Mn-Cr-Sn in the $L2_1$ structure, we calculated the changes in the total energy as a function of lattice parameter. Energy curves were computed for different magnetic reference states (FM and FIM ones).

The variation of total energy for different magnetic reference states of 16-atom supercells studied is shown in Fig. 3(a–c). The equilibrium total energies for different magnetic reference states for supercells #1, #2 and #3 is shown in Fig. 3(d).

We found that different supercells have different magnetic reference states. It can be seen from Fig. 3(a) that for supercell #1 the FM spin configuration in austenite is energetically favorable compared to FIM configurations, while in a case of the supercell #2 the FIM-II spin configuration in austenite is energetically favorable. Finally, for supercell #3 the FIM-III spin configuration in austenite is energetically favorable. It can also be seen that the FIM-II order of the supercell #2 has a lower energy in comparison to other magnetic configurations of both supercells #1 and #3. This indicates clearly that supercell #2 is the stable atomic configuration in the austenitic phase of $Ni_7Co_1Mn_5Cr_1Sn_2$. It should be noted that to estimate the optimized lattice constants for all alloys studied, we fitted the dependences of total energy on a cell volume according to the Birch-Murnagahan equation of state. The equilibrium lattice parameters for supercells #1, #2 and #3 are equal to 5.971 Å, 5.951 Å and 5.952 Å, respectively.

In order to investigate the trend for martensitic deformation, we

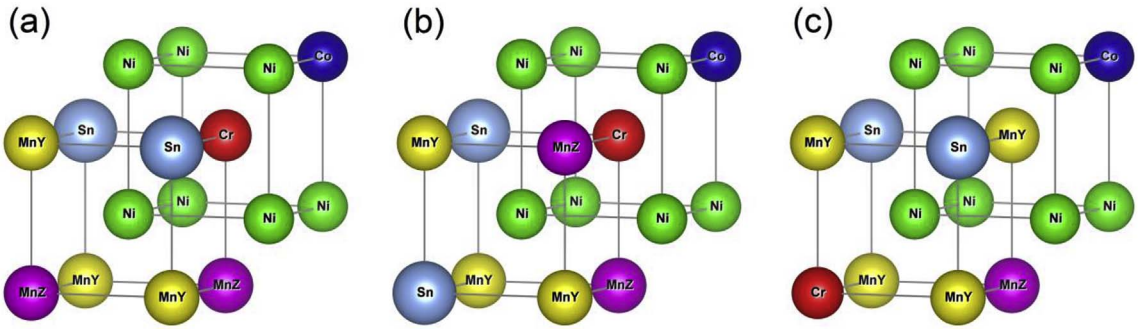

Fig. 1. 16-atom supercells of $Ni_7Co_1Mn_5Cr_1Sn_2$ with different atomic distribution relative to Cr atom. a) supercell #1; b) supercell #2; c) supercell #3. (For interpretation of the references to colour in this figure legend, the reader is referred to the web version of this article.)